Correlation between Fatigue of Automotive Wheel Centre — Discs and Hour-glass Laboratory Specimen

P.J. McGrath[a], D.G. Hattingh[b] and M.N. James[c]

Fatigue testing of complete automotive wheels is carried out on rotary bend machines. These commercial machines simulate hard-cornering conditions and mainly test the fatigue performance of the central section of an automotive wheel[1]. This paper develops a relationship for predicting the fatigue performance of the wheel, based on fatigue tests of hourglass specimens machined from centre discs. This is more economical of material and, in principle, also allows the effect on fatigue performance of change in production parameters or starting alloy to be assessed, by considering a limited number of wheel blanks taken from each stage of the production process. This is potentially a very useful tool in optimising material selection, wheel design and production parameters. The particular centre-disc under consideration is manufactured from a dual-phase steel (DPS)[2]. Good correlation was achieved between S-N data from the automotive wheels and that from the hourglass (HG) specimens.

NOMENCLATURE

S-N – Stress-Life
HG – Hour-glass
R-value – Stress Ratio value
S_a = Stress amplitude
S_{max} = S_a - under zero mean stress conditions
N_f = Number of fatigue cycles to failure

Introduction

Fatigue durability testing[1] of automotive wheels is carried out on complete wheels, i.e. integral units comprising of the wheel rim with attached centre-disc in the finished, painted condition. The production process for the centre-disc involves a series of stamping operations on an initially blank plate, while the rim is made via a sequence of rolling operations. Once the rim and the centre-disc have passed through their respective manufacturing processes, they are assembled, degreased, painted and finally cured at a temperature of around 190°C.

Fatigue strength of finished wheels are assured by random selection of samples for fatigue testing, and results assessed in fatigue durability terms by determining whether or not the samples meet the minimum life specifications under a given applied bending moment[3]. For this specific wheel fracture occurs along a circumferential axis just inside the cup radius region (see Figure 1c), where a change in material thickness is observed. Relatively small changes in wheel design, material specification and production process are known to induce premature fatigue failures, but there is currently no way of assessing the effect of these parameters a priori. Thus changes in design and initial press tooling are implemented in an iterative fashion, by the manufacturing and testing of complete wheels.

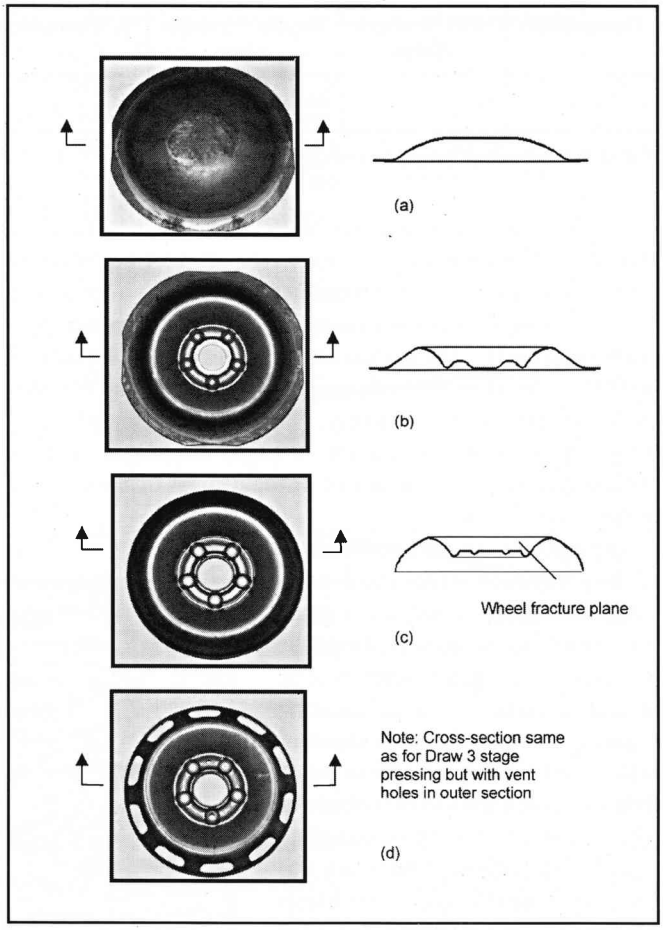

Figure 1: Production stages of a wheel; a) Draw 1 stage pressing; b) Draw 2 stage pressing; c) Draw 3 stage pressing; d) Venting stage

Material

The centre-discs are manufactured from a dual-phase steel 2 (DPS600 is the wheel manufacturers designation), whose specified chemical composition and mechanical properties are given in Tables 1 and 2 respectively. The microstructure of this steel and having a grain size of ASTM 12 is shown in Figure 2.

Fatigue testing

Complete automotive wheels were tested on a commercial

[a] Department of Mechanical Engineering, Technikon Pretoria, Private Bag X680, Pretoria, South Africa, 0001.
E-mail: mcgrathp@techpta.ac.za
[b] Department of Mechanical Engineering, Port Elizabeth Technikon, Private Bag 6011, Port Elizabeth, 6000.
[c] Department of Mechanical and Marine Engineering, University of Plymouth, Plymouth PL 4 8AA, Devon, United Kingdom.

Chemical Symbol	C	Mn	P	S	Si	Al	Cr	Ni	Mo	Ti	Cu
% Composition	0.05 0.12	0.5 1.3	0.01 0.09	Max 0.006	Max 0.65	0.02 0.06	Max 0.9	Max 0.25	Max 0.05	Max 0.015	Max 0.35

Table1: Chemical composition of DPS600 material

Designation	Yield Strength (MPa)	Tensile Strength (MPa)	% Elongation
DPS600	427	664	28

Table 2: Mechanical properties of DPS600 material

rotary-bend fatigue-testing machine (Figures 3 and 4) and the HG specimens were tested in reverse bending on a laboratory fatigue-testing machine. Commercially there are two conditions that determine the minimum required fatigue performance (S-N curve) of wheels[3]. For this particular wheel, tests must survive 60 000 cycles at an applied moment of 2750 Nm and 600 000 cycles at 1800 Nm respectively. The stress state in a wheel by these applied moments cannot be easily calculated, and includes an unknown influence of residual stress on mean stress in the fatigue cycle.

In particular, it is not known which of the production stages involved in wheel manufacture are most detrimental to fatigue life. It would be useful for wheel manufacturers to be able to ascertain such information reliably and quickly from standard fatigue tests, and to be able to relate data from such tests to that obtained from durability testing of complete wheels. The purpose of this work was to examine the relevance of such tests for a particular dual-phase steel used in the manufacture of a wheel for a passenger vehicle, and to develop a relationship between S-N data from HG specimens and from complete wheels.

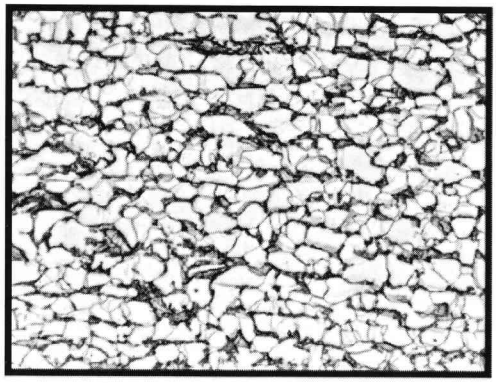

Figure 2: Microstructure of DPS600 x 500

Thus, in order to simulate the above test conditions using laboratory specimens, it was necessary to establish the maximum tensile principal stresses induced in the wheel under commercial testing practice and to replicate these stresses in the HG specimen. This was achieved by applying strain rosettes to the wheel (see Figure 5) and testing the instrumental wheel in a cantilever-bending fatigue-testing machine as shown in Figure 4. As both cantilever and rotary bending induce similar surface stress states (R values similar), results from both types of test are comparable.

Strain rosettes on the wheel were applied parallel to, at 45° to, and transverse to the rolling direction (RD) of the steel plate (see Figure 5). The wheel was then rotated by hand applying a range of loads to the wheel during the period it was mounted in the cantilever-bend testing machine. These loads spanned the two industrially relevant loads (2750 Nm and 1800 Nm) and are given in Table 3, together with the calculated maximum principal stresses as assessed in the three directions, i.e. parallel to, 45 deg. to and transverse to the RD of the sheet plane. The maximum tensile principal stress data from the 45° direction in the wheel, referenced to the rolling direction, were used for fatigue testing the HG specimens – see Table 3. Not only are these stresses the most amenable to simple linear modelling of the relationship between maximum tensile principal stress S_{max} and applied moment M but they also indicate the greatest maximum stress value. These stresses (from the 45 ° direction) are shown plotted against the applied test moments in Figure 6, where the mean stress values are fairly constant at around 27 MPa. The following equation describes this relationship:

$$S_{max} = 0.0589 \times M + 14.88 \; (MPa) \qquad (1)$$

In order to obtain slightly conservative results (in terms of fatigue life prediction) from the fatigue testing of HG specimens, the applied mean load was taken as zero. Considering a Goodman-type mean stress correction to stress amplitude, the mean stress/tensile stress ratio is only some 0.166%. This difference may be regarded as negligible when applied to critical components such as vehicle wheels.

At least four wheels were tested on the rotary bend testing machine by the manufacturer at each of the following values of applied moment: 1800, 2420, 3375 and 4000 Nm, which were chosen to span the two specification test values of 2750 Nm and 1800 Nm. HG fatigue specimens machined from finished wheels (see Figure 7) were tested at the maximum principal stress values that were equivalent to moments of 2125 Nm through to 4000 Nm. The lower value of 2125 Nm produced lives > 2×10^6 cycles, which was taken as representing the endurance limit (run-out) – see Figure 9.

HG fatigue specimens were also machined from centre-disc blanks taken from intermediate production stages. The manufacturer supplied only a limited number of these discs (which are illustrated in Figure 1). Hence a fatigue life

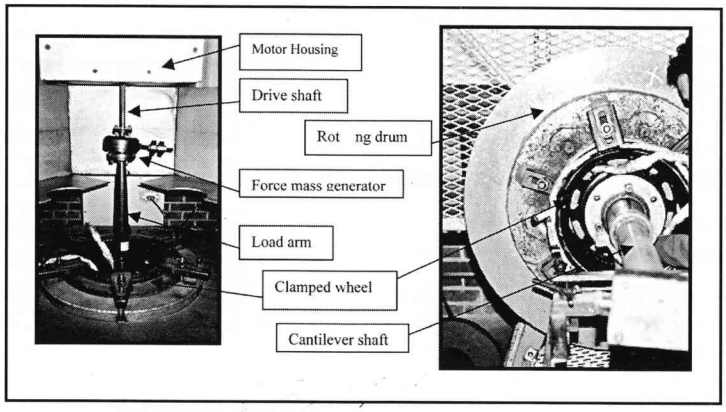

Figure 3: Rotary bending fatigue testing machine

Figure 4: Cantilever-type rotary bending fatigue testing machine

Applied Moment in Wheel Test (Nm)	Max. Prin. Ten. Stress (MPa)	Max. Prin. Comp Stress (MPa)	Mean Stress (MPa)
1500	79	-52	14
2125	62	-110	-24
2750	93	-136	-22
3375	154	-153	1
4000	244	-177	34
Applied Moment in Wheel Test (Nm)	**Max. Prin. Ten. Stress (MPa)**	**Max. Prin. Comp Stress (MPa)**	**Mean Stress (MPa)**
1500	103	-38	33
2125	140	-91	25
2750	179	-119	30
3375	210	-169	21
4000	252	-198	27
Applied Moment in Wheel Test (Nm)	**Max. Prin. Ten. Stress (MPa)**	**Max. Prin. Comp Stress (MPa)**	**Mean Stress (MPa)**
1500	62	-110	-24
2125	89	-126	-19
2750	143	-160	-9
3375	177	-193	-8
4000	219	-226	-4

Table 3: Assessed Principle Stresses for RD (top), 45 degree to RD (middle) and Transvers to RD (bottom)

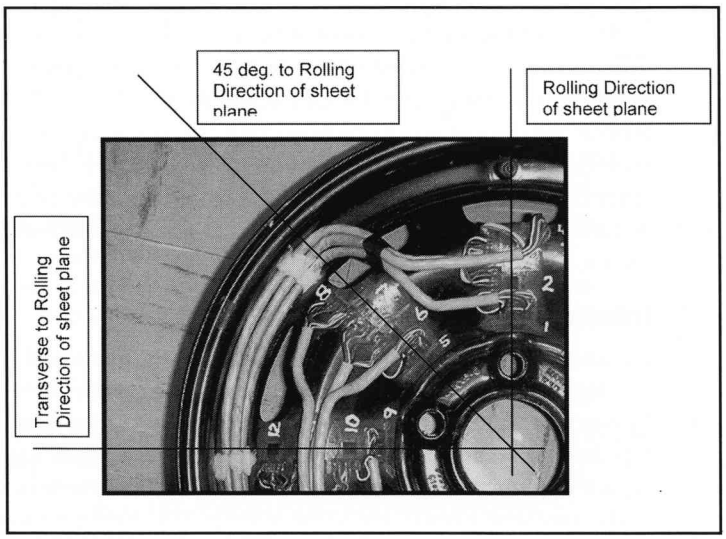

Figure 5: Section of guaged wheel used for assessing the maximum tensile principal stresses

comparison between the various production stages was possible only at a single value of stress, which was chosen to be the highest stress value, i.e. 252 MPa, in order to minimize scatter in the data, which tends to increase at longer lives. Whilst not being optimal, this represents the most efficient use of the limited number of specimens and should give indication of the fatigue behaviour of production stage components. As with the finished wheel specimens, the fracture plane observed during testing of a complete wheel was maintained in these laboratory specimens through suitable design and manufacture, where this was possible, i.e. for Draw 2 and 3 stage pressings as well as for the venting stage. The fracture plane in the blank and Draw 1 stage pressing was not chosen to coincide with any particular circumferential position.

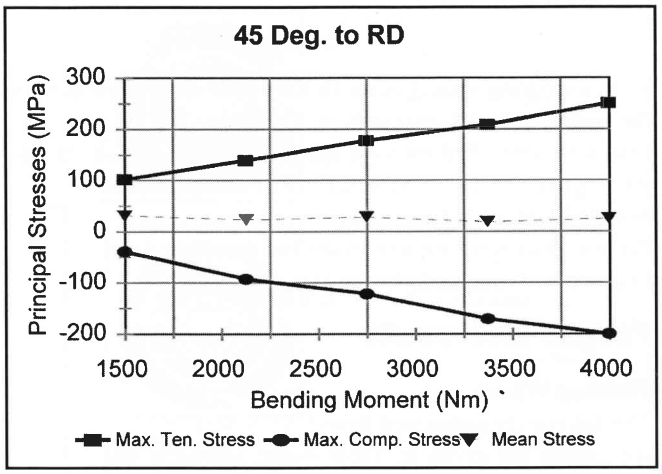

Figure 6: Maximum principal stresses and mean stress variation with applied moment

Specimen Preparation

When testing complete wheels no preparation was necessary prior to conducting the fatigue tests. For the case of the laboratory specimens, however, centre-discs were in the first instance sectioned from the wheel rim and the HG specimens then machined using a CNC milling machine, this is shown in Figure 7. As mentioned above, where possible the narrowest part of the HG shape was chosen to coincide with the circumferential plane along and through which fracture occurs under industrial fatigue testing conditions. The relative size of the wheel centre-disc and fatigue specimens allowed eight specimens to be machined from a centre-disc (Figure 7). However, the wheel geometry (vent and stud holes) meant that, from Draw 2 stage pressing, only five of these were considered suitable for fatigue testing. The remaining three specimens contained unwanted notches in the cup radius region as a result of the odd number of stud holes.

These fatigue specimens reflect the curvature of the centre-disc. Hence their ends were not parallel to one another, and were not in the same horizontal plane when placed in the fatigue-testing machine in an orientation equivalent to that observed in the wheel. It was therefore necessary to provide a flat seating at either end of the specimen to ensure correct orientation of the specimen when mounted in the fatigue-testing machine. An illustration of the HG testing parameters is indicated in Figure

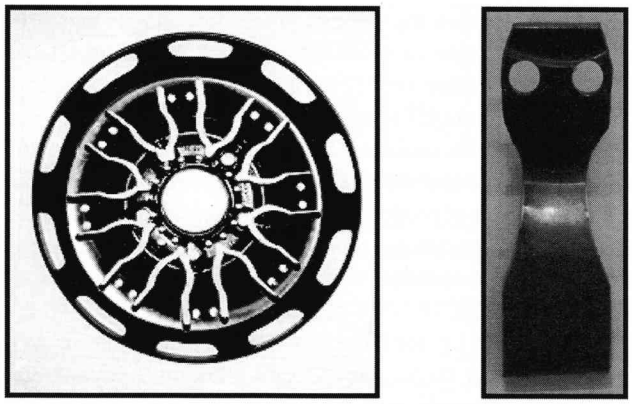

Figure 7: Centre disc as machined into H-G shaped fatigue specimens, on the right a typical H-G specimen as removed from the machined disc

8. A cold curing resin (Lecoset 7007) was therefore cast around the ends in a mould, as is indicated in Figure 8. The applied test load was controlled through specimen strain, measured via a strain gauge attached to the surface of the specimen. For the blank and Draw 1 stage pressing specimens, these problems were not relevant, but the applied test load was still controlled via a strain gauge.

Fatigue test results

Finished Wheels

The fatigue data obtained from both wheel and HG specimens are given in Table 4 and represent the average of several tests, as previously mentioned. Note that the average fatigue lives marked (*) pertaining to the wheel data are interpolated values, while the value marked (**) is an extrapolated value. These interpolated values were obtained using equation (2), which best describes the fatigue performance of the wheel (in terms of equivalent peak tensile stress, S_a (equal to S_{max} in the case where the mean stress is zero).

Applied Moment in Wheel Test (Nm)	Max. Ten. Prin. Stress Amplitude (MPa)	Cycles to Failure HG Specimen (N_f)	Cycles to Failure Wheels (N_f)
4000	252	104 900	72 500
3375	210	245 500	180 700
2750	179	610 500	483 900*
2420	—	—	847 900
2125	140	>2 000 000	1 255 800*
1800	—	—	1 980 200
1500	103	—	2 610 400**
Note: For meaning of * and ** see text			

Table 4: Wheel and HG fatigue results (Note: $2x10^2$ cycles is considered run-out)

$$S_a = -35.2 \times \ln N_f + 639.23 \ (MPa) \qquad (2)$$

The above equation indicates that when $N_f = 0$, $S_a \approx$ tensile strength. This implies that when the intercept is equal to the tensile strength of the material, failure will occur in one quarter of the first fatigue cycle [4,5,6], which is physically justifiable. Figure 9 indicates the trends for the HG specimen and wheel fatigue curves, compared with the manufacturer's minimum life specification for the wheel. HG specimen data were not obtained at the equivalent peak tensile stress amplitude of 103 MPa, since run-out (defined as $N_f > 2 \times 10^6$ cycles) was observed to occur at the 140 MPa test load level. The dotted line in Figure 9 is an extension of the curve to indicate run-out at 2×10^6 cycles. Using the curves in this figure, the fatigue performance of the wheel may be approximated with the following relationship:

$$N_{f(wheels)} = 0.74x \ N_{f(HG\ specimens)}$$

The agreement between the wheel data and HG specimen data is really very good, and correlates well with the expected

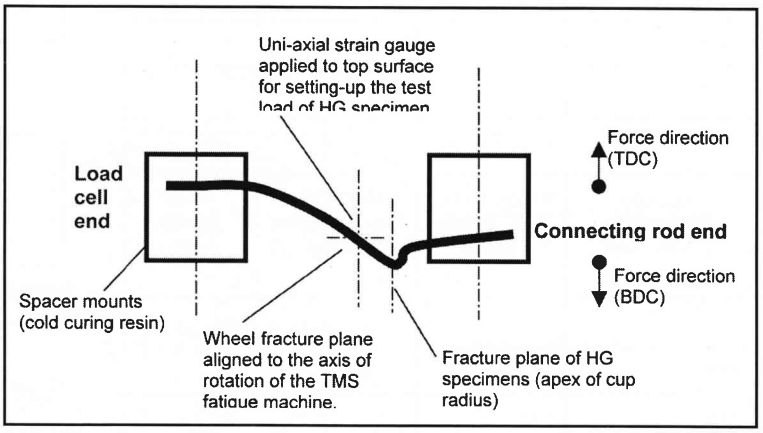

Figure 8: Schematic illustration of HG fatigue testing parameters

variation from a 40 MPa difference in mean stress values in the two types of test (the HG specimen data being slightly conservative). Typical fracture features of HG specimens are shown in Figures 11 and 12. It therefore seems clear that HG specimen data could be used to predict the life of vehicle wheels when changes in either design, or material, or both, are contemplated.

This could be further extended by linking stress data from finite element analysis of wheel designs with a database of fatigue curves for potential wheel materials. This would then provide the desired result of a predictive capacity of optimum choices prior to commencing any tooling manufacture. Over a range of wheel designs and materials, it seems that there could be considerable cost savings with testing efficiency inherent in such a system.

Intermediate Production Stages

It is also of some interest to establish which of the manufacturing stages might be considered detrimental to fatigue life. Table 5 gives the results of four fatigue tests at each production stage, together with the mean value and percentage decrease in life. Figure 10 plots the mean value of life. It is clear that there is a fairly consistent trend of reduction in fatigue life through each production stage, with the largest reduction in fatigue resistance being recorded after the first pressing stage (Draw 1) and

Prod. Stage	Spec. 1	Spec. 2	Spec. 3	Spec. 4	Cycles to Failure N_f	Decrease in Fatigue Life %
Blank	1013900	753700	1398500	1056300	1055600	0
Draw 1	*	177200	177700	—	177500	83
Draw 2	110700	102500	126200	124600	116000	36
Draw 3	112900	113100	107500	117400	112800	3
Venting	109600	98800	99600	*	102700	9
FPW	97600	59900	52500	69900	70000	32

Table 5: Fatigue data of production stage HG specimens at S_a = 252 MPa

after the assembly, painting and curing of the wheel.

Life therefore seems to reflect the amount of plastic deformation sustained by the wheel during its forming, rather than the increase in tensile strength. This is attributed to the formation of micro-voids[7] at martensite/ferrite boundaries (see Figures 13 and 14) during the pressing operations, and which were observed in the microstructure of components after the Draw 1 stage pressing. These would tend to circumvent the crack initiation stage and reduce the fatigue life of such work-hardened steel components. The reduction in life observed after assembly, painting and baking, is interesting and is attributed to carbo-nitrides[1], which occurs during the baking treatment.

Conclusions

The following conclusions can be drawn regarding the fatigue life of vehicle wheels as determined at various production stages:

- Good correlation has been achieved between the fatigue data obtained from hourglass specimens and from the testing of complete wheels. Fatigue life can therefore be predicted from S-N testing of HG specimens cut out from full production wheels.
- The fatigue life decreases through the various production stages due to plastic deformation and work hardening. This leads to the formation of micro-voids in the steel, which act as crack initiation sites. The most detrimental stages in the production of a wheel are the first pressing stage (Draw 1 stage pressing) and the final assembly, painting and curing phase.
- The possibility exists to combine such data with a finite element analysis and predict wheel performance in advance of commencing manufacture, when either design modifications or a change of material is proposed.

Acknowledgements

The authors acknowledge the assistance received from members of the Manufacturing Technology Research Centre, and from the technical staff of the Department of Mechanical Engineering, PE Technikon, in preparing and machining the HG specimens from the wheel discs. Guestro Wheels (Eastern Cape Division), South Africa, is thanked for supplying the wheel discs and for their assistance with fatigue testing of wheels.

References

1. Mizui, M., Sekine, T. and Soneda, S. Application of High Strength Steel Sheets for Automotive Wheels, Society of Automotive Engineers, *No. 850540, 1985, pp. 1 – 13.*

2. Mizui, M. and Takahashi, M. High Strength Steels for Automotive Wheels, Mechanical Working Steel Process (MWSP) Conference, *29, 1992, pp. 57 – 64.*

3. Technischer Uberwachungs Verein (T ü V) Technote, Regulation for the Testing of Special Wheels for motorcars, motorbikes and Trailers, 1995, pp.1 - 24.

4. Suresh, S. Fatigue of Materials, *Cambridge University Press, 1991.*

5. Bannantine, J. et al., Fundamentals of Metal Fatigue Analysis, *Prentice-Hall Inc., 1990.*

6. Collins, J. Failure of Materials in Mechanical Design, *Second Edition, John Wiley & Sons, 1993, ISBN 0 471 55891 5.*

7. Wei, DC. Rim section fatigue results of various HSLA steel wheels, ASME *International Conference on Advances in* Life Prediction Methods, *1983, pp.285 – 291.*

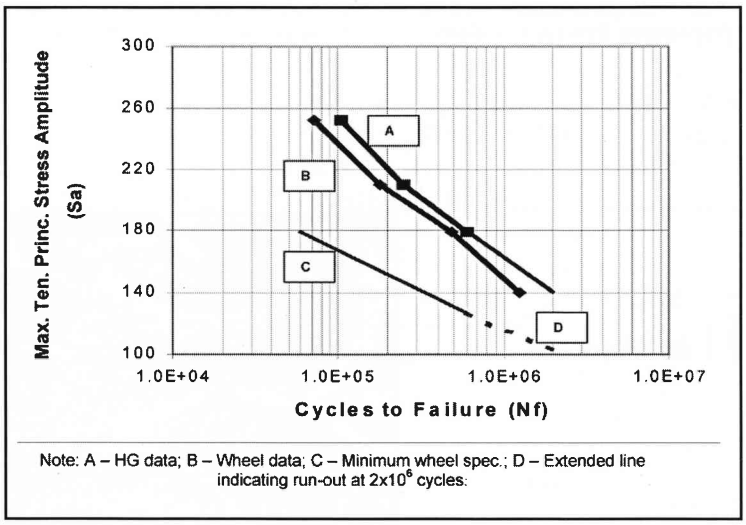

Figure 9: Comparison between wheel, HG and maximum wheel specification

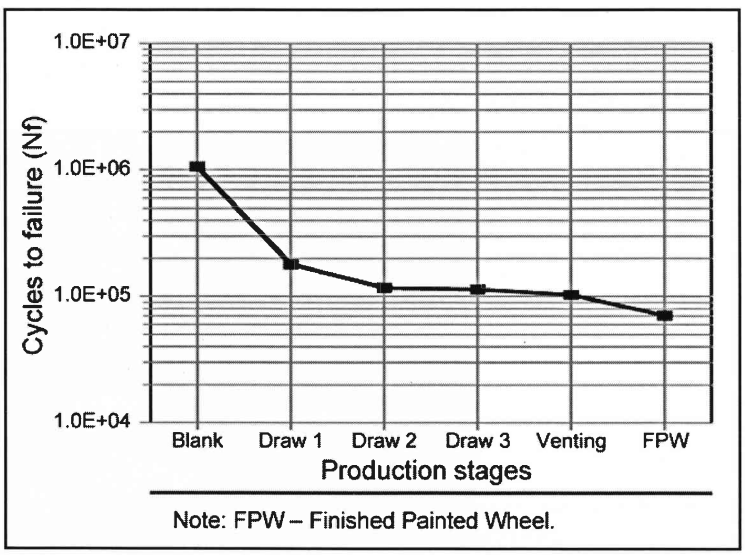

Figure 10: Fatigue performance of production stage specimens

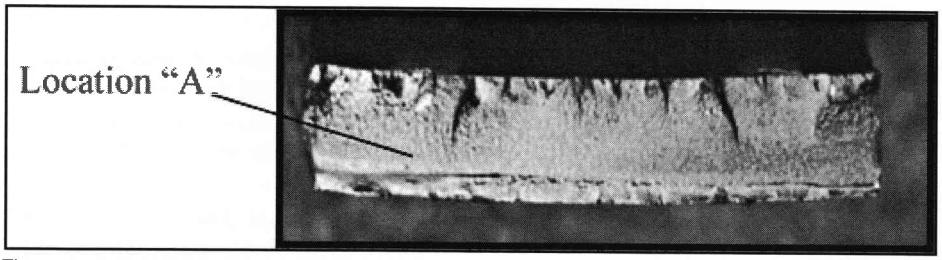

Figure 11: Typical Features of HG specimens

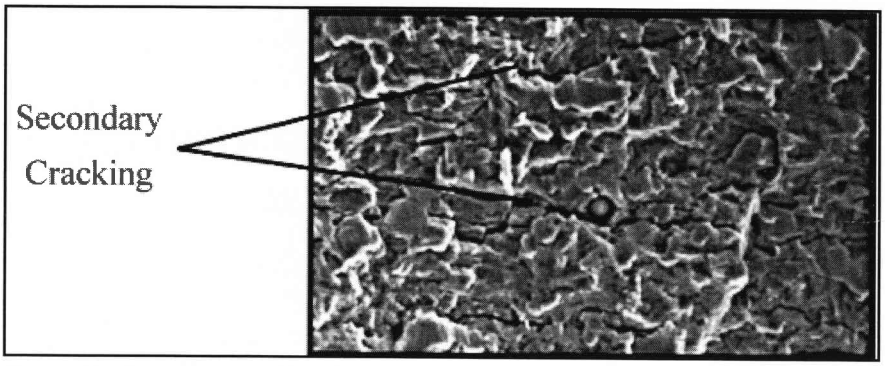

Figure 12: Secondary cracking (location "A" in figure 12) effects resulting from crack propagation through the elastic core (stress discontinuity) region x775

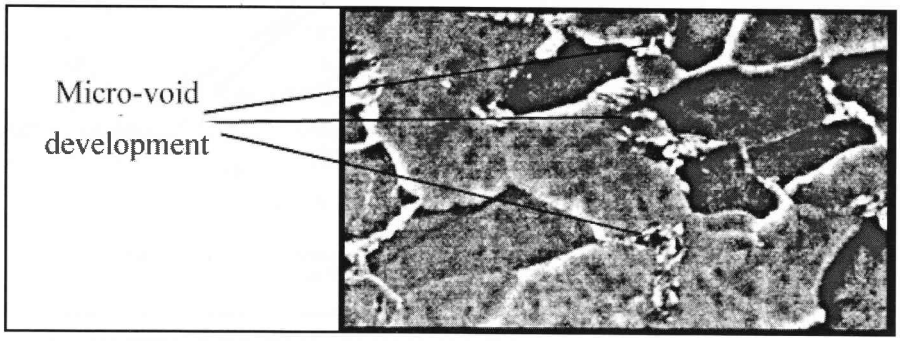

Figure 13: Microstructure of Draw 1 stage pressing x3865

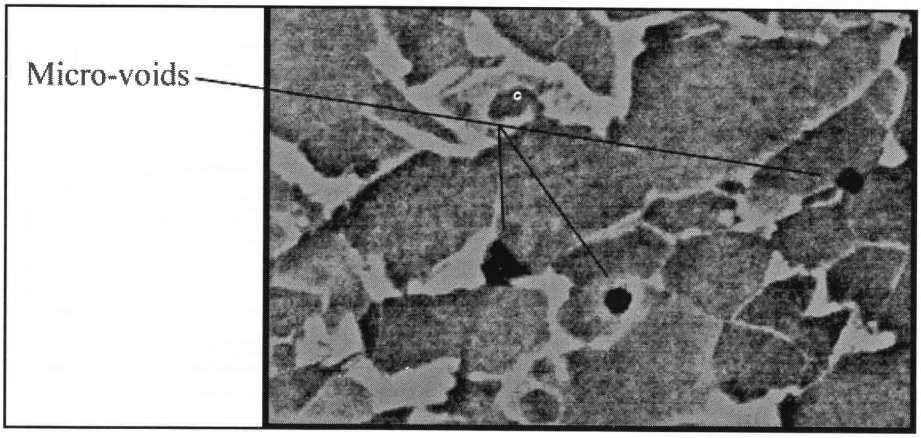

Figure 14: Micro-voids close to the inside surface of the cup radius region x3865